Advanced electron microscopy techniques for studying ice and firn cores

I. Baker,[1] K. Sieg,[1] N. Spaulding,[2] and D. Meese[1,2]

[1]Thayer School of Engineering, Dartmouth College, Hanover, NH 03755 (Ian.Baker@Dartmouth.edu) (Katherine.E.Sieg@Dartmouth.edu)
[2]Climate Change Institute, University of Maine, Orono, ME 04469 (Nicole.Spaulding@Maine.edu) (Debra.Meese@Maine.edu)

Summary For many years, the microstructural characterization of ice and firn has used optical microscopy often involving observation of thin sections between crossed polarizers. However, such an approach, in addition to being of low resolution, does not provide complete information on the microstructure. In previous work (Obbard et al. 2003), we have shown how scanning electron microscopy coupled with X-ray microanalysis can be used to determine the microstructural location of impurities in ice cores. In this paper, we outline the use of scanning electron microscopy-based techniques to determine the 3-D orientation of grains and, thus, enable more complete analysis of the orientation relationships between grains in ice and firn. In addition, we show how scanning electron microscopy can be used to determine the internal surface area, porosity and grain size in firn.

Citation: Baker, I., K. Sieg, N. Spaulding, and D. Meese (2007), Advanced electron microscopy techniques for studying ice and firn cores: *in* Antarctica: A Keystone in a Changing World – Online Proceedings of the 10th ISAES, edited by A.K. Cooper and C.R. Raymond et al., USGS Open-File Report 2007-1047, Extended Abstract 185, 4 p.

Introduction

The technique commonly used to characterize grain structures in ice is inspection of a thin (0.5-1 mm) section of ice between crossed polarizers when, due to the optical birefringence of ice, grains of dissimilar orientations appear with different colors. This birefringence is also utilized for determining the orientation of the *c*-axis of ice grains using a Rigsby universal stage, which consists of four rotation axes, a specimen mount and two crossed polarizers. In careful hands, the Rigsby stage can be used to obtain *c*-axis directions accurate to 5° (Rigsby, 1951; Langway, 1958) - an excellent description of the use of the stage is available in Wilen et al. (2003). In the last few years, this optical technique has been automated by a number of different groups (Yang and Azuma, 1999; Russell-Head and Wilson, 2001; Wilen, 2000; Hansen and Wilen, 2002), as described in Wilen et al. (2003), making it not only more rapid but also improving its accuracy to ~1°. While the automated technique is a significant improvement, it still only provides the *c*-axis direction, i.e. it does not provide the complete 3-D orientation.

Recently, we utilized electron backscatter diffraction (EBSD) in a scanning electron microscope (SEM) to measure the full 3-D orientations, i.e. both the *c*-axis and *a*-axis directions, of grains in polycrystalline ice with both high angular (0.5^{o}) and spatial (50 nm) resolution (Iliescu et al. 2004; 2005; Obbard et al. 2006, 2007). (The shape and orientation of etch pits on the surface of ice (Matsuda, 1979: Matsuda and Wakahama, 1978) and x-ray diffraction (e.g. Mori and others, 1985) can also be used to obtain both the *c*-axis and *a*-axis orientations of ice, albeit rather slowly.) Knowing the full 3-D orientations of grains is particularly useful for analysis of the misorientations between neighboring grains, and, hence, for distinguishing between (migration) recrystallization and polygonization. Further, the technique can be used to produce orientation images of grains, and particularly subgrains, in which optical contrast between (sub)grains may not be sufficient to differentiate them. In addition to providing images and orientation information, with the use of an energy dispersive X-ray spectrometer, the microstructural location of soluble impurities can be ascertained and the compositions of dust particles obtained (Cullen and Baker 2000; 2001; 2002a; 2002b; Cullen et al. 2002; Iliescu et al. 2002; Baker et al. 2003; Baker and Cullen 2003a; 2003b; Obbard et al. 2003a; 2003b; Iliescu and Baker 2004; Baker et al. 2006; Barnes et al. 2002a; 2002b; 2003; Mulvaney, Wolff and Oates 1988; Wolff, Mulvaney and Oates 1988).

In addition to examining ice cores, crystal structure examination of cores of firn provides possibly the most valuable insight into the processes by which firn is transformed into glacial ice. Recently, we have demonstrated that we can examine firn in an SEM to determine the grain size and orientation, the internal surface area and porosity, and we can determine the microchemistry of the firn (Baker et al 2007a, 2007b). This technique has several advantages over the usual techniques of infiltrating the firn with a liquid. For example, dodecane has been used as a pore filler to obtain grain size, but alters the firn structure and can be confused with grains, particularly when using automated imaging systems. Dimethyl phthalate (Albert and Shultz 2002; Rick and Albert 2004) is also used to obtain pore size by allowing the liquid to set, and then sublimating the firn. The problems with the latter methods are that the viscous liquid cannot easily penetrate small pores, which increase in frequency with depth; the liquid cannot infiltrate closed off pores, which also increase in frequency with depth; and there is the issue of how much the liquid changes the local structure of the firn during solidification. Additionally, all of these liquids are hazardous at some level.

In this paper, we briefly describe the use of SEM-based techniques that we applied to the determination and analysis of the orientations of grains in ice and firn cores, and for the characterization of the pore structure in firn.

Experimental methods

Typically, for SEM examination specimens of dimensions ~25mm × 25mm × 10mm thick were cut perpendicular to the core axis, shaved flat with a razor blade under a HEPA-filtered, laminar-flow hood at -10°C and frozen onto a brass plate. Specimens were then either sealed in a small container for later examination or mounted onto a cold stage for immediate observation.

For both secondary electron imaging and acquisition of EBSD patterns, uncoated specimens were examined in a field emission gun (FEG) FEI XL-30 environmental SEM. For acquisition of EBSD patterns, a pre-tilted (25°) coldstage was used, see Figure 1. The pre-tilt was necessary because the geometrical set-up of the SEM would only allow the stage to be tilted by 45°, and a 70° specimen tilt is needed to maximize the weak signal used for producing EBSD patterns.

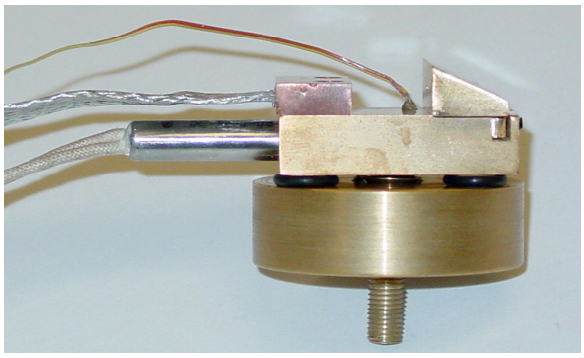

Figure 1. SEM cold stage showing the pre-tilted stage used for EBSD determination. The copper braid used for cooling, the cartridge heater used for heating, and the thermocouple are connected to the stage on the left.

Our previous home-built, cold stages were cooled by nitrogen gas that had passed through a liquid nitrogen heat exchanger (Obbard et al. 2003a). The temperature of the stage was determined by the flow rate of the nitrogen gas. Such a set-up cools rapidly and the temperature can be easily controlled to within ± 5°C. However, it has the disadvantage that a nitrogen gas leak can cause problems in the SEM, particularly a FEG SEM. Also, using concertina-type stainless steel tubing for the nitrogen gas makes stage movement difficult and exerts significant torque on the SEM motor-driven stage. The current set-up, shown in Figure 1, utilizes a copper braid connected to an external liquid nitrogen reservoir to cool the specimen stage. A PID-controlled cartridge heater, with a thermocouple for feedback, is used to provide heating to maintain a specific temperature. This set-up avoids the possibility of a nitrogen leak into the SEM chamber and the torque on the SEM stage motor and maintains the temperature well. Its disadvantage is that the cool-down time is quite long compared to the previous set-up (1 h versus 15 mins).

The SEM was operated at 15 kV with a beam current of 0.15 nA under a pressure of ~5 x 10^{-4} Pa, and the ice was maintained at -80°C ± 10°C. EBSD patterns were captured using the techniques described by Iliescu et al. (Iliescu et al. 2004; 2005) and indexed using HKL Technologies' CHANNEL 5™ software.

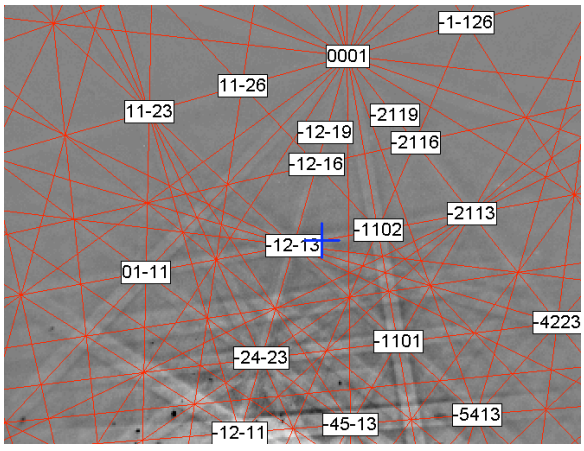

Figure 2. EBSD pattern from an ice core specimen. The red lines are drawn in the center of the Kikuchi bands and the major poles, where several Kikuchi bands intersect, are indexed. The blue cross indicates the pattern center. Hence, the specimen normal is close to $\left[\bar{1}2\bar{1}3\right]$.

Results and discussion

Figure 2 shows an EBSD pattern produced from an ice core. The pattern was produced by simply stopping the scanning electron beam on a point of interest, and collecting the diffraction pattern produced by back-scattered electrons on a nearby phosphorescent screen.

Figure 3 shows pole figures constructed from EBSD patterns, such as that shown in Figure 2, obtained from 391 grains in an ice core specimen from a depth of 727 m at Siple Dome, Antarctica. The traditional Rigsby stage analysis would have provided only the *c*-axis pole figure shown on the left, which indicates a single maximum. The EBSD patterns provide complete 3-D orientation data and, hence, the *a*-axis pole figure shown on the right was also obtained. The latter pole figure shows clusters of poles, often in lines. Correlation with the specimen from which the EBSD patterns were obtained showed that these grains were generally quite close to each other. The small misorientations between the grains suggested that the specimen had undergone significant polygonization.

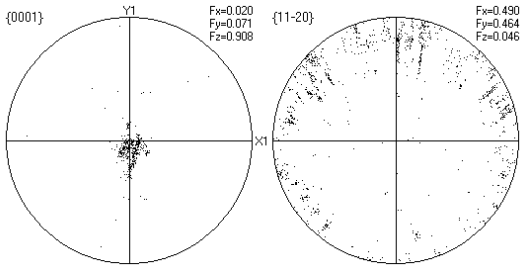

Figure 3. *c*- and *a*-axis pole figures constructed from EBSD patterns from 391 grains from a depth of 727 m at Siple dome, Antarctica.

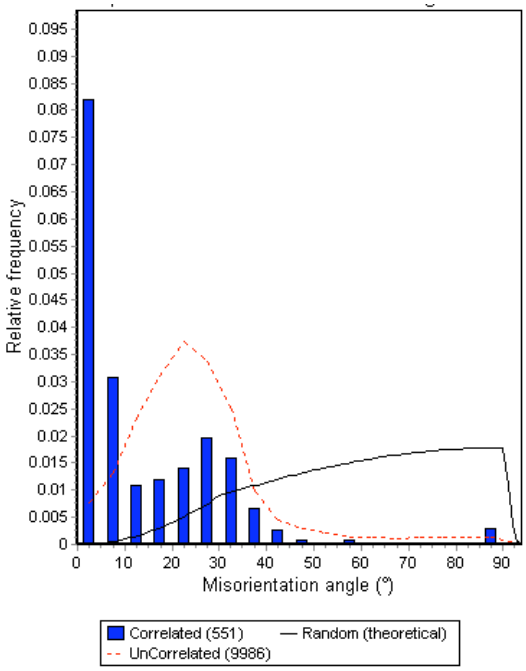

Figure 4. Frequency of misorientation angles between grains for the 391 grains from 727 m Siple dome ice. The correlated misorientations, which are from adjacent grains, show a high frequency of low angle boundaries. The solid curve is for a theoretical random distribution of grain orientations.

The presence of many small angle grain boundaries is made more evident in a plot of frequency versus misorientation angle between adjacent (correlated) grains. This is shown in Figure 4, where it is clear that the frequency of low-angle grain boundaries is far greater than random, again indicating that many of the grains were probably formed by polygonization following deformation. Such an analysis is not possible using *c*-axis data alone since even when the *c*-axes from two adjacent grains are in the same direction, the two grains could be rotated by 30° with respect to each other.

Figure 5 shows both a thin-section optical photograph, produced using the standard dodecane pore-filler technique, and a secondary electron image of 16-meter deep samples from core ITASE02-1. In Figure 5(a), the red arrow indicates pore filler. Note that the filler appears to overtake some crystals making the determination of grain size difficult and that no clear estimation of the relationship between grain and pore can be made.

In Figure 5(b), the red arrow marked GB points to a grain boundary. One example of a pore is marked with "pore" in red. Note that in some locations, such as in the lower right-hand corner, the 3-dimensional aspect of the grain can be visualized. Analysis of images, such as that shown in Figure 5(b), using the pixel-counting measurement utility of the program Image SXM (Barrett 2005) enables the internal surface area and porosity to be determined. Imaging of grain boundary grooves (see arrowed example in Figure 5(b)), formed after allowing the specimen to sublimate, enables the grain size of the firn to be determined. A key observation from this SEM imaging is that the features referred to as "grains" based on the optical microscopy technique (analogous to grains of sand) are not actually individual crystals or grains, but in fact consist of multi grains. Thus, the grain size determined from the SEM-based technique is significantly smaller than that obtained from the optical microscopy-based technique (Spaulding, et al., 2007).

The use of the SEM also allows high-resolution images of bonds between snow particles that formed the firn to be obtained. Microchemical information can also be obtained from the firn using X-ray microanalysis (Baker et al., 2007a, 2007b).

Conclusions

In this paper, we have attempted to show the utility of using scanning electron microscope-based techniques for examining ice cores and firn cores. It has been shown that, compared to "traditional" methods, not only may additional information, such as *a*-axis orientations be obtained, which enables more sophisticated analyses of the grain orientations to be performed, but that some traditional methods, e.g. the pore-infiltration optical thin-section technique for examining firn, may give incorrect results.

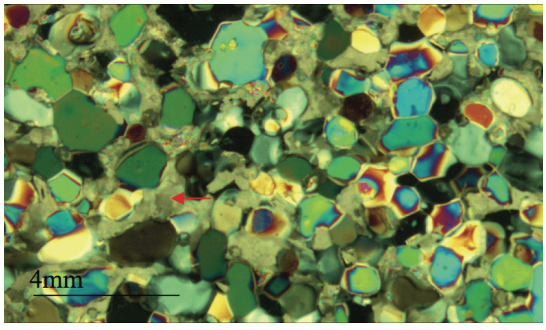

(a)

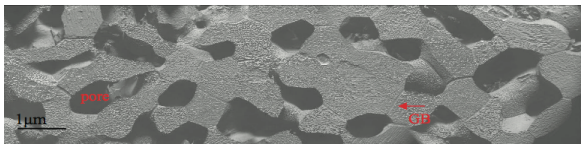

(b)

Figure 5. (a) Thin-section optical photograph of dodecane pore-infiltrated firn, and (b) secondary electron image of firn, both from a depth of 16-meter from core ITASE02-1.

Acknowledgements. Support by the U.S. National Science Foundation Office of Polar Programs Grants 0440523 (Dartmouth College), 0636483 and 0538494 (University of Maine) is gratefully acknowledged. The views and conclusions contained herein are those of the authors and should not be interpreted as necessarily representing official policies, either expressed or implied, of the National Institute of Standards and Technologies, or the U.S. Government.

References

Albert, M., and E.F. Shultz (2002), Snow and firn properties and air-snow transport processes at Summit, Greenland, Atmospheric Environment, 36, 2789-2797.

Baker, I., and D. Cullen (2003a), The Structure and Chemistry of 94m GISP2 ice, Annals of Glaciology, 35, 224-230.

Baker, I., and D. Cullen (2003b), SEM/EDS observations of impurities in polar ice: artifacts or not? Journal of Glaciology, 49, 184-190.

Baker, I., D. Cullen and D. Iliescu (2003), The microstructural location of impurities in ice, Canadian Journal of Physics, 81, 1-9.

Baker, I., D. Iliescu, R. Obbard, H. Chang, B. Bostick, and C.P. Daghlian (2006), Microstructural Characterization of Ice Cores, Annals of Glaciology, 42, 441-444.

Baker, I., R.W. Obbard, D. Iliescu and D. Meese (2007a), "Microstructural Characterization of Firn", Proceedings of the 63rd Eastern Snow Conference, Newark, DE, p211-218.

Baker, I., R.W. Obbard, D. Iliescu and D. Meese (2007b), "Microstructural Characterization of Firn", Hydrological Processes, in press.

Barnes, P.R.F., R. Mulvaney, K. Robinson and E.W. Wolff (2002a), Observations of polar ice from the Holocene and the glacial period using the scanning electron microscope, Annals of Glaciology, 35, 559-566.

Barnes, P.R.F., R. Mulvaney, E.W. Wolff and K. Robinson (2002b), A technique for the examination of polar ice using the scanning electron microscope, Journal of Microscopy 205, 118-124.

Barnes, P.R.J., E.W. Wolff, D.C. Mallard, and H.M. Meider (2003), SEM Studies of the Morphology and Chemistry of Polar Ice, Microscopy Research and Technique, 62, 62-69.

Barrett S. 2005. Image SXM, Surface Science Research Centre, University of Liverpool, Liverpool, UK.

Cullen, D., and I. Baker (2000), The Chemistry of Grain Boundaries in Greenland Ice, Journal of Glaciology, 46, 703-706.

Cullen, D., and I. Baker (2001), Observation of Impurities in Ice, Microscopy Research and Technique, 55, 198-207.

Cullen, D., and I. Baker (2002a), Sulfate Crystallites in Vostok Accretion Ice, Materials Characterization, 48, 263-270.

Cullen, D., and I. Baker (2002b), Scanning Electron Microscopy of Vostok Accretion Ice, in Proceedings of Microscopy and Microanalysis, 1546-7CD.

Cullen, D., D. Iliescu and I. Baker (2002), SEM/EDS Studies of Impurities in Natural Ice, in Proceedings of Microscopy and Microanalysis, 1398-9CD.

Hansen, D. P., and L. A. Wilen (2002), Performance and applications of an automated c-axis ice-fabric analyzer, Journal of Glaciology, 48, 159-170.

Iliescu, D., I. Baker and D. Cullen (2002), Preliminary Microstructural and Microchemical Observations of Pond and River Accretion Ice, Cold Regions Science and Engineering, 35, 81-99.

Iliescu, D., and I. Baker (2004), Characterization of the microstructure and mechanical properties in seasonal lake and river ice, in Proc. 24th Army Science Conference, Orlando, FL, OS-26.

Iliescu, D., I. Baker and H. Chang (2004), Determining the Orientations of Ice Crystals using Electron Backscatter Patterns, Microscopy Research and Technique, 63, 183-187.

Iliescu, D., I. Baker and C.P. Daghlian (2005) Orientation Mapping in Polycrystalline Ice Using Electron Backscatter Patterns, in Proceedings of Microscopy & Microanalysis, Honolulu, HI, 1500-1501.

Langway, C. C. Jr. (1958), Ice fabrics and the universal stage, SIPRE Tech Rep, 62, 1-16.

Matsuda, M., and G. Wakahama (1978), Crystallographic structure of polycrystalline ice, Journal of Glaciology, 21, 607-620.

Matsuda, M. (1979), Determination of a-axis orientations of polycrystalline ice, Journal of Glaciology, 22, 165-169.

Mori, Y., T. Hondoh and A. Higashi (1985), Development of an automatic ice fabric analyzer, Annals of Glaciology, 6, 281-283.

Mulvaney, R., E.W. Wolff and K. Oates (1988), Sulphuric acid at grain boundaries in Antarctic ice, Nature, 331, 247-249.

Obbard, R., D. Iliescu, D. Cullen, J. Chang and I. Baker (2003a), SEM/EDS Comparison of Polar and Seasonal Temperate Ice, Microscopy Research and Technique, 62, 49-61.

Obbard, R., D. Iliescu, I. Baker and D. Cullen (2003b), A Technique for the Scanning Electron Microscopy and Microanalysis of Uncoated Ice Crystals, in Electron Microscopy: Its Role in Materials Science, The Mike Meshii Symposium, TMS, Warrendale, PA, 133-140.

Obbard, R., I. Baker and K. Sieg (2006), Using Electron Backscatter Diffraction Patterns To Examine Recrystallization in Polar Ice Sheets, Journal of Glaciology, 52, 546-557.

Obbard, R., and I. Baker (2007), The Microstructure of Meteoric Ice from Vostok, Antarctica, Journal of Glaciology, 53, 41-62.

Rick, U., and M. Albert (2004), Microstructure of West Antarctic Firn and its Effect on Air Permeability, ERDC/CREEL Report, TR-04-16.

Risby, G.P. (1951), Crystal Fabric Studies on Emmons Glacier, Mount Rainier, Washington, Journal of Glaciology, 59, 596-598.

Russell-Head, D. S., and C.J.L. Wilson (2001), Automated fabric analyzer system for quartz and ice, Geol. Soc. Aust. Abstracts, 64, 159.

Spaulding, N., D. Meese and I. Baker (2007), Determination of polar firn/ice core physical properties using scanning electron microscopy, 37th Annual Arctic Workshop, Skaftafell, Iceland, May 2nd – 5th.

Wilen, L.A., C.L. DiPrinzio, R.B. Alley and N. Azuma (2003), Development, Principles, and Applications of Automated Ice Fabric Analyzers, Microscopy Research and Technique, 62, 49-61.

Wilen, L. A. (2000), A new technique for ice fabric analysis, Journal of Glaciology, 46, 129-139.

Wolff, EW, R. Mulvaney and K. Oates (1988), The location of impurities in Antarctic ice, Annals of Glaciology, 11, 194-197.

Yang, Y., and N. Azuma (1999), A new automated ice-fabric analyzer which uses image analysis techniques, Annals of Glaciology, 29, 155-162.